Multiple magnetic states and irreversibilities in the Fe_xTiS_2 system

N. V. Selezneva,[1] N. V. Baranov,[1,2] E. M. Sherokalova,[1] A. S. Volegov,[1,2] and A. A. Sherstobitov[1,2]
[1]*Institute of Natural Science and Mathematics, Ural Federal University, Ekaterinburg 620083, Russia*
[2]*M.N. Miheev Institute of Metal Physics, Ural Branch of the Russian Academy of Science, Ekaterinburg 620108, Russia*

(Received 10 May 2021; revised 21 June 2021; accepted 28 July 2021; published 6 August 2021)

The structural and concentration conditionality of magnetic states and transport properties of layered chalcogenide compounds Fe_xTiS_2 ($0 \leqslant x \leqslant 0.75$) have been studied by means of x-ray and neutron diffraction, magnetization, electrical resistivity, and magnetoresistance measurements performed on polycrystalline samples synthesized by solid-phase reaction method with prolonged homogenization heat treatment. It has been revealed that various magnetic states [spin-cluster glass state at $x < 0.25$, antiferromagnetic (AFM) order at $x \approx 0.25$–0.28, cluster glass state at $x \approx 0.33$, AFM at $x \approx 0.45$–0.5, and ferrimagnetic ordering above $x = 0.5$] are realized in the Fe_xTiS_2 system with increasing Fe content. The absence of a long-range magnetic order in $Fe_{0.33}TiS_2$ is confirmed by neutron diffraction measurements. The magnetic states observed in this system are closely related not only to the concentration of Fe atoms, but also, to a greater extent, to their distribution over the cation layers. It is assumed that the single crystals obtained by chemical vapor deposition are practically unique objects with only their inherent properties, which leads to inconsistency between the literature data on the magnetic properties of these compounds. Changes in the magnetic state of Fe_xTiS_2 with Fe concentration are accompanied by nonmonotonic dependencies of the magnetoresistance and coercivity with maximal absolute values in compounds with the AFM virgin state. The ferrimagnetic order in compounds with $x > 0.5$ is suggested to originate in Fe-Ti mixing in cationic layers. The AFM ordered compounds undergo the field-induced phase transitions to the metastable high-coercive ferromagnetic (FM) state, which is accompanied by a large remnant magnetoresistance. The enhanced coercivity observed in compounds with the AFM virgin state is ascribed to the intrinsic exchange bias together with the Ising-type spin state of Fe ions.

DOI: 10.1103/PhysRevB.104.064411

I. INTRODUCTION

Transition metal dichalcogenides MX_2 with a layered crystal structure where hexagonal layers of transition (M) metal are sandwiched between two hexagonal layers of chalcogen (X) atoms are attracted relentless interest owing to the rich variety of unusual properties and potential applications [1–5]. The difference in layer stacking in MX_2 leads to the formation of materials with variety of possible polytypes: 1T structure (trigonal symmetry and trigonal antiprismatic coordination); 2H structure (hexagonal closed packing, trigonal prismatic coordination); and 3R structure with rhombohedral symmetry, which leads to significant discrepancies in the electronic structure of materials and their properties [6]. While transition metal and chalcogen atoms in the X-M-X triple layers are bonded by strong ion-covalent bonds, these sandwiches in bulk materials are coupled by weak van der Waals (vdW) forces. On the one hand, due to the weak coupling between X-M-X sandwiches, the MX_2 crystals can be exfoliated to single-layer or multilayer nanosheets exhibiting unusual physical and electronic properties that differ from their bulk parent samples [4,5]; and, on the other hand, foreign M' atoms can be inserted (intercalated) into such vdW gaps giving new bulk M'_xMX_2 materials with significantly modified properties [6–10]. Most bulk MX_2 compounds with NiAs type structures exhibit paramagnetic properties in normal state [7], however, the intercalation of M' atoms having a magnetic moment leads to the appearance of spin-glass or cluster-glass magnetic states at $x < 0.25$, or various long-range magnetic orderings in M'_xMX_2 with higher intercalant concentrations [8–18]. The conductivity of the M'_xMX_2 intercalation compounds (M = Ti, V, Ta, Nb, V) is mainly of metallic type [19,20]. The Ruderman-Kittel-Kasuya-Yoshida (RKKY) type exchange interaction through conduction electrons, superexchange interaction via chalcogen atoms and Dzyaloshinskii-Moriya interaction [8,21–23] are considered as mechanisms leading to different magnetic orderings in M'_xMX_2 depending on the type and concentration of M' atoms as well as on the type of a parent compound MX_2. The site-occupation disorder of M' atoms within layers and local competition between exchange interactions were suggested to be important factors affecting the magnetic properties of M'_xMX_2 as well [24,25]. These frustrations are apparently responsible for the large (up to ~50%) spread in the magnetic ordering temperatures observed in highly intercalated compounds with close compositions; for example, the Curie temperatures from 160 [12] to ~69 K [26] were reported for the Fe_xTaS_2 compounds with Fe concentrations $x = 0.25$–0.28; for the ferromagnetic compound $Cr_{0.33}NbSe_2$, the Curie temperature determined by different authors varies from 82 K up to 115 K (see Ref. [17] and references therein).

Such discrepancies in properties of the highly intercalated M'_xMX_2 apparently originate in differences in sample preparation methods and conditions. However, not only the magnetic ordering temperatures of M'_xMX_2, but also the arrangement of magnetic moments in the subsystem of intercalated M' atoms, the magnetic state and magnetization behavior of the compounds are observed to depend on the preparation methods, annealing and cooling conditions as well. As published by different authors, the $Cr_{0.33}NbS_2$ compound may exhibit a helimagnetic structure [27] or ferromagnetic (FM) ordering [28]. As for impact of the Fe intercalation into MX_2 structures, most Fe_xMX_2 compounds (M = Ti, V, Ta, Nb; X = S, Se) with Fe concentrations $x = 0.25$, 0.33 and 0.5 are reported to have an antiferromagnetic (AFM) order [8,11,13–15,29–33] although in Fe_xTaS_2 with Fe concentrations $0.20 < x < 0.35$, the well-defined FM order was observed [12,34]. The presence of AFM ordering in the selenide compounds Fe_xTiSe_2 at $0.25 \leqslant x \leqslant 0.5$ was evidenced by the susceptibility measurements [33,35], neutron diffraction [11] and high-field magnetization data [15]. In contrary to other Fe_xMX_2, there is a significant scatter in data reported in literature regarding the magnetic state and physical properties of the highly intercalated ($x \geqslant 0.25$) sulfide Fe_xTiS_2 samples prepared by different methods. According to Ref. [36] vacancy ordered $Fe_{0.5}TiS_2$ ($FeTi_2S_4$) single crystals, grown at 1173 K using chlorine as a growth agency, show an AFM behavior below the Neel temperature 138 K. The existence of AFM ordering in $Fe_{0.5}TiS_2$ with a well-ordered monoclinic crystal structure was confirmed by neutron diffraction measurements [13,14] on powder samples synthesized by solid-state reactions. In addition, the presence of an AFM ground state and the formation of the field-induced FM state in $Fe_{0.5}TiS_2$ was supported by the magnetoresistance data [13,15]. The observation of a large remnant magnetoresistance in a polycrystalline $Fe_{0.25}TiS_2$ sample [18] with ordered Fe atoms was ascribed to presence of an AFM virgin state in this compound as well. The large magnetoresistance observed in the antiferromagnetically ordered $Fe_{0.5}TiS_2$ and $Fe_{0.25}TiS_2$ compounds was attributed to the superzone boundary effects [13,15,18,37]. However, it should be also noted that according to the recently published work [16], the Fe_xTiS_2 single crystals grown using iodine vapor transport at a temperature gradient of 1173–1073 K exhibit the FM state coexisting with glassy behavior in the entire Fe concentration range $0.1 \leqslant x \leqslant 0.7$, although in some previous studies [9], the formation of the FM state in Fe_xTiS_2 was proposed only above $x = 0.4$. The magnetic state of Fe_xTiS_2 at high Fe concentrations (above $x = 0.5$) also seems to be an open question, since the magnetic order and transport properties in the highly intercalated Fe_xTiS_2 can be affected by mixing of Fe and Ti ions in adjacent cationic layers [38].

Bearing in mind the inconsistencies encountered in studies of Fe_xTiS_2 the present work aims to determine the key factors responsible for changes in the magnetic state in this system with increasing Fe concentration up to $x = 0.75$. Published data regarding the Fe_xTiS_2 system indicate that physical properties of these compounds, especially at high intercalant concentrations and in single-crystalline form, are strongly dependent on the distribution and orderings of Fe atoms in the lattice. Therefore, in this study, we focused on the study of the crystal structure, magnetic and transport properties on the polycrystalline Fe_xTiS_2 samples obtained by the solid-state reaction method with prolonged homogenization heat treatment. Since the electrical resistivity of these compounds turned out to be very sensitive to changes in their magnetic state with intercalation, temperature and under the influence of a magnetic field, we also carried out detailed studies of the magnetoresistance behavior. Along with magnetic measurements and neutron diffraction, the magnetoresistance data allowed us to reveal various magnetic states, irreversible phase transformations, and build an updated magnetic phase diagram.

II. EXPERIMENT

Polycrystalline Fe_xTiS_2 samples ($x = 0$–0.75) were synthesized by the two-stage solid-phase reaction method, as already described [13]. The starting materials were small pieces of 99.95% pure titanium, sulfur (99.99%) and powder of iron (purity 99.98%). At first, the parent compounds TiS_2 was synthesized inside a sealed quartz tubes by heat treatment of a mixture of starting materials at 800 °C for one week. At the second stage, the mixtures of Fe and TiS_2 powders were pressed into tablets and annealed at the same conditions. The obtained specimens were milled, then compacted and homogenized for two to four weeks at 800 °C followed by cooling down through removal of the tube from the oven into air. Structural characterization of the obtained samples was done using a Bruker D8 Advance x-ray diffractometer with Cu K_α radiation and the FULLPROF software package. Neutron powder diffraction measurements for $Fe_{0.33}TiS_2$ were performed with wavelength $\lambda = 2.45$ Å by means of the focusing powder diffractometer E6 installed at the Helmholtz-Zentrum Berlin. The temperature dependencies of the electrical resistivity of Fe_xTiS_2 were measured by a four-probe dc method in the temperature range from 8 up to 300 K with using a closed-cycle refrigerator on parallelepiped samples with sizes of about of $2 \times 2 \times 8$ mm^3 made from tablets. The measurements of the electrical resistivity in magnetic fields up to 100 kOe were performed by a four-contact ac method by using a cryo-free DMS-1000 system (Dryogenic Ltd, UK). The measurements of the magnetic susceptibility and magnetization were performed by means of a Quantum Design SQUID MPMS magnetometer in the temperature interval $2\ \text{K} \leqslant T \leqslant 350$ K.

III. RESULTS

A. Crystal structure

Our analysis of the powder x-ray diffraction (XRD) data for Fe_xTiS_2 samples showed that intercalation leads to a change in interatomic distances and the appearance of different superstructures due to the ordering of Fe atoms in layered NiAs-type structures. The XRD patterns for Fe_xTiS_2 compounds with various Fe concentrations are presented in Fig. 1. The samples with low intercalant concentrations ($x < 0.20$) are observed to exhibit the same trigonal crystal structure of the CdI_2 type as the parent compound TiS_2 (space group $P\bar{3}m1$), which indicates that Fe atoms located between the triple S-Fe-S layers are not ordered and distributed

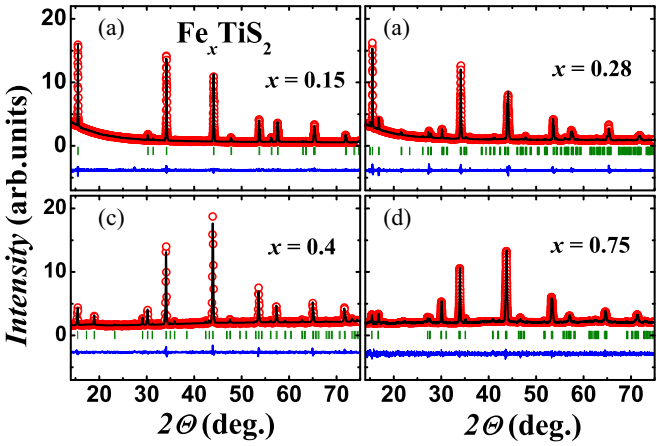

FIG. 1. Observed (symbols) and calculated (lines) x-ray diffraction pattern for Fe_xTiS_2 samples with various Fe concentrations. Vertical bars indicate the Bragg peaks positions corresponding to the $P\bar{3}m1$ space group in the case of $x = 0.15$, $C12/m1$ space group for $x = 0.28$, $P\bar{3}1c$ for $x = 0.4$, and $I12/m1$ for $x = 0.75$. The difference between calculated and observed intensities is shown in the bottom.

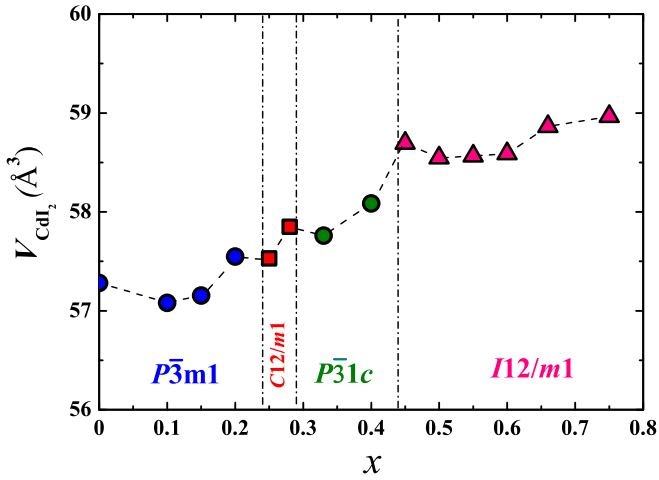

FIG. 2. Changes in the unit cell volume of the CdI_2 type structure and space groups with increasing Fe content in Fe_xTiS_2. The errors are within the symbol sizes.

randomly. At $x = 0.2$, small additional reflections are observed in the XRD pattern indicating the appearance of ordering $2a_0 \times 2a_0 \times 2c_0$ (space group $P\bar{3}m1$), where a_0 and c_0 are the concentration-dependent lattice parameters of the CdI_2 type unit cell. According to recently published electron microscopy data [39,40], long-range order is absent in $Fe_{0.2}TiS_2$ single crystals, although some regions with an ordered $(2 \times 2 \times 2)$ arrangement of Fe atoms are observed.

An increase in the Fe content up to $x = 0.25$ leads to the formation of Fe chains and the appearance of monoclinicity. The crystal structure of $Fe_{0.25}TiS_2$ is of the M_5X_8 type and can be considered as the superstructure $2\sqrt{3}a_0 \times 2a_0 \times 2c_0$ belonging to the space group $C12/m1$, which is in good agreement with results of previous structural studies of $Fe_{0.25}TiS_2$ by x-ray [18,41] and neutron diffraction [42] measurements. The same ordering is observed at $x = 0.28$ (Fig. 1). Note that there are some contradictions in the literature regarding the type of superstructure that is realized in $Fe_{0.25}TiS_2$; the formation of the $\sqrt{3}a_0 \times \sqrt{3}a_0$ [16] and $2a_0 \times 2a_0$ [40] orderings was revealed in single crystalline samples by means of transmission electron diffraction and microscopy techniques. Such a discrepancy may occur due to differences in sample preparation procedures, in particular, in synthesis temperatures and cooling conditions.

The Bragg peaks on diffraction patterns for the Fe_xTiS_2 compounds with Fe contents $0.28 < x \leqslant 0.4$ are indexed in the trigonal singony (space group $P\bar{3}1c$), which is associated with the emergence of the triangular network and $\sqrt{3}a_0 \times \sqrt{3}a_0 \times 2c_0$ superstructure of the M_2X_3 type. These x-ray data are consistent with electron microscopy results for the $Fe_{0.33}TiS_2$ crystals [40]. Further intercalation of Fe up to $x = 0.45$ leads to the formation of the monoclinic $\sqrt{3}a_0 \times a_0 \times 2c_0$ superstructure of the M_3X_4 type (space group $I12/m1$) with reduced distances between Fe chains; the same superstructure is observed for the compounds with Fe contents within $0.5 \leqslant x \leqslant 0.75$. As a result, a sequence of structural changes $CdI_2 \rightarrow M_5X_8 \rightarrow M_2X_3 \rightarrow M_3X_4$ is observed with increasing concentration of Fe atoms due to a change in their distribution over the lattice.

Figure 2 displays the changes in the reduced volume V_{CdI2} of the primitive unit cell of the CdI_2 type structure with increasing iron content in the Fe_xTiS_2 system. As can be seen, the V_{CdI2} value is nearly constant up to $x = 0.20$, while further growth of the intercalant content leads to the expansion of the crystal lattice with some kink in the vicinity $x = 0.5$. It should be noted that the monoclinicity appeared in the vicinity of $x = 0.25$–0.28 and at $x \geqslant 0.45$ results from distortions of the hexagonal arrangement of S and Ti ions in *ab* plane owing to the formations of Fe chains. It seems that such distortions are rather difficult to detect in electron microscopic studies of single crystals.

As follows from neutron diffraction measurements performed for the Fe_xTiS_2 compounds with $x \leqslant 0.5$ [13,14,42,43], iron atoms occupy octahedral positions between S-Ti-S tri-layers randomly at $x < 0.25$ and in an ordered manner at $0.25 \leqslant x \leqslant 0.5$. However, at Fe concentrations higher than $x = 0.5$, some mixing of Fe and Ti ions in neighboring cationic layers may occur; part of iron atoms can occupy positions in titanium layers, while titanium atoms can be placed in the vdW gap between sandwiches along with iron atoms. Note that the absence of full cation partitioning was revealed by neutron diffraction in the vanadium disulfide-based compound FeV_2S_4 ($Fe_{0.5}VS_2$) [44].

B. Magnetic susceptibility and magnetization

Figure 3 shows, as an example, the results of the magnetic characterization of the $Fe_{0.1}TiS_2$ sample. The temperature dependence of the magnetic susceptibility [Fig. 3(a)] measured at $H = 1$ kOe under zero-field cooling (ZFC) and field-cooling (FC) modes shows anomalous behavior below the freezing temperature $T_f \approx 27$ K (shown by the vertical arrow), which can be associated with the formation of a cluster glass (CG) magnetic state. Our T_f value is close to ~30 K previously reported for this composition [45,46]. The inverse susceptibility shown in Fig. 3(b) can be described above

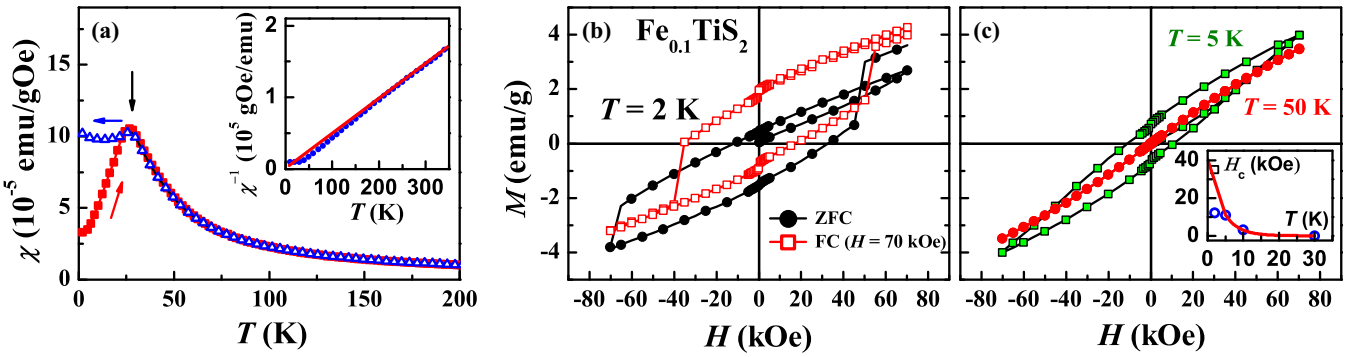

FIG. 3. Magnetic susceptibility (a) measured at $H = 1$ kOe in ZFC and FC regimes versus temperature and field dependencies of the magnetization [(b) and (c)] measured at various temperatures on a $Fe_{0.1}TiS_2$ sample. Insets show the inverse susceptibility and the coercive field versus temperature.

~180 K by the expression $\chi(T) = \chi_0 + C/(T - \theta_p)$, where χ_0 is the temperature independent contribution and the second term is the Curie-Weiss (CW) contribution. However, when the temperature decreases below 180 K, the $\chi^{-1}(T)$ dependence shows a downward deviation from the high-temperature straight line corresponding to the CW behavior, which can be attributed the presence of the short-range magnetic correlations (clusters) in the paramagnetic region. The paramagnetic Curie temperature θ_p for $Fe_{0.1}TiS_2$ was estimated to be about of 5 K, which is significantly lower that T_f value (27 K), and indicates that both the AFM and FM exchange interactions exist in this compound with a slight predominance of the FM exchange. Fitting the $\chi^{-1}(T)$ dependence in the temperature range 180–350 K to the CW law allowed us to estimate the effective magnetic moment per Fe atom as $\mu_{\text{eff}} \approx 3.7\mu_B$, which is lower than spin-only value $\mu_{\text{eff}} = 4.89\ \mu_B$ expected for Fe^{2+} ion apparently due to involvement of Fe $3d$ electrons in the formation of the covalent-like bonds and hybridization of Fe $3d$ states with Ti $3d$ and S $3p$ electronic states. It should be noted, that the 2+ valence state of Fe ions in Fe_xTiS_2 with Fe concentrations up to $x \approx 0.5$ and the presence of the Fe $3d$ - Ti $3d$ hybridization are evidenced by x-ray spectroscopy studies [47,48]. The large magnetization jumps and asymmetric $M(H)$ dependencies are observed at 2 K [Fig. 3(b)] after zero-field cooling and after cooling at $H = 70$ kOe from 150 K in contrast to the open symmetric hysteresis loop at $T = 5$ K [Fig. 3(c)]. The ZFC $M(H)$ dependence is shifted downward, while the $M(H)$ loop obtained at 2 K after cooling at 70 kOe is biased upward along the magnetization scale. These low-temperature $M(H)$ dependencies imply the inhomogeneity of the magnetic state and the presence of competing exchange interactions in $Fe_{0.1}TiS_2$. Note, the shift of the hysteresis loops along the magnetization axis was observed in systems with coexisting AFM and FM interactions and phases [49,50]. As follows from Fig. 3(b), the $Fe_{0.1}TiS_2$ compound has a very high coercive field ($H_c \sim 35$ kOe) after cooling in a field of 70 kOe, and, as expected, an increase in temperature leads to a decrease in the H_c value [shown in the inset in Fig. 3(c)]. As to the magnetization jumps, such a stair-case behavior of the magnetization with the field was also detected at low temperatures in Fe_xTiS_2 with higher Fe concentrations (see below).

As we have recently shown [18], an increase in the Fe concentration up to $x = 0.25$ together with the formation of the $2\sqrt{3}a_0 \times 2a_0 \times 2c_0$ superstructure (see above) results in substantial changes in the magnetic behavior of the compound. In contrast to the CG behavior of $Fe_{0.1}TiS_2$, the $Fe_{0.25}TiS_2$ compound was observed to exhibit several features characteristic for highly anisotropic magnets: a large difference between FC and ZFC curves below ~52 K, almost rectangular hysteresis loop and huge coercive field ($H_c \sim 40$ kOe at 2 K). However, a combined study of the magnetic and transport properties of $Fe_{0.25}TiS_2$ allowed us to assume that this compound exhibits an AFM virgin state below $T_N \sim 52$ K and undergoes a field-induced phase transition into a metastable FM state [18].

As can be seen in Fig. 4, nearly the same magnetization behavior is observed in the compound $Fe_{0.28}TiS_2$ with a slightly higher Fe content; although, in contrast to $Fe_{0.25}TiS_2$, the compound with $x = 0.28$ the temperature dependence of the susceptibility shows an anomaly at ~59 K, bifurcation of the ZFC and FC curves with decreasing temperature and a pronounced hump around 40 K. At 2 K, an increase in the magnetic field applied to a sample cooled in zero field to a value of about 35 kOe leads to a sharp increase in the magnetization; and the magnetization reversal of this sample with further changes in the field occurs through magnetization jumps at a coercive field $H_c \sim 21$ kOe, which shows that the initial magnetization curve is outside the hysteresis loop. As the temperature rises, the curves become smooth and the coercive force decreases [see Figs. 4(b) and 4(c)].

As for $x = 0.25$ [18], the $H_c(T)$ dependence above 5 K for $Fe_{0.28}TiS_2$ can be well fitted by exponential law: $H_c(T) = H_c(0)\exp(-\alpha T)$ [solid line in the inset in Fig. 4(c)]. As will be shown below, taking into account the data on magnetoresistance, the magnetic state of $Fe_{0.28}TiS_2$ can be characterized as inhomogeneous, consisting of an AFM matrix with inclusions of clusters with short-range magnetic correlations. It is worth to mention that in $Fe_{0.28}TiS_2$, as well as in compounds with lower Fe concentrations, the inverse susceptibility does not obey the CW law in the entire temperature range above magnetic critical temperature, and the $\chi^{-1}(T)$ dependence start to deviate downward from the straight line when the temperature decreases below ~200 K. We attributed such a behavior in $Fe_{0.25}TiS_2$ [18] to the presence of a Griffiths-like phase [51,52] in the nominally paramagnetic state since the subsystem of the Ising-type Fe atoms located between S-Ti-S sandwiches can be considered as diluted with vacancies

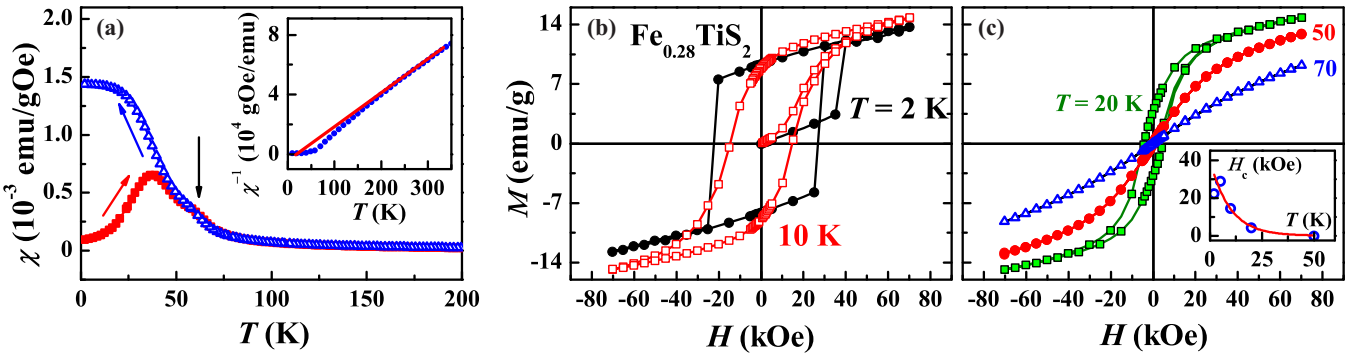

FIG. 4. Temperature dependencies of the magnetic susceptibility measured in ZFC and FC regimes (a) and field dependencies of the magnetization measured at various temperatures [(b) and (c)] measured on a $Fe_{0.28}TiS_2$ sample. The vertical arrow indicates the magnetic critical temperature. Insets show the $\chi^{-1}(T)$ dependence (a) and H_c vs T dependence (c).

that makes the Fe_xTiS_2 compounds quite compatible with the Griffiths model [51]. In the temperature range between the critical temperature T_{crit} and certain temperature T_G (Griffiths temperature) corresponding to the Curie temperature of the ideal (undiluted) system, the the inverse magnetic susceptibility $\chi^{-1}(T)$ varies with temperature as $(T/T_{crit}-1)^{1-\lambda}$, where λ is the magnetic susceptibility exponent [53]. For $Fe_{0.25}TiS_2$ [18], a value of λ was estimated as 0.757 which is consistent with $0 \leqslant \lambda < 1$ for the Griffiths phase [53].

As follows from Fig. 5(a), the magnetic susceptibility of the $Fe_{0.33}TiS_2$ compound shows the large difference between ZFC and FC curves below ~44 K (indicated by the vertical arrow); and the deviation of the inverse susceptibility below 200 K from the straight line is observed as well [see inset in Fig. 5(a)]. This compound exhibits a higher value of the paramagnetic Curie temperature ($\theta_p \approx 44$ K) compared with $Fe_{0.25}TiS_2$ ($\theta_p = 34$ K [18]), and a value of μ_{eff} is estimated as 3.9 μ_B. Unlike steplike $M(H)$ dependencies observed at low temperatures for the samples with $x = 0.25$ and 0.28, the magnetization isotherms for $Fe_{0.33}TiS_2$ show quite smooth behavior [Figs. 5(b) and 5(c)] even at 2 K with substantially reduced H_c values ($H_c \sim 7.5$ kOe at $T = 2$ K). Note, that this value of the coercive field is close to H_c obtained for single-crystalline samples of $Fe_{0.33}TiS_2$ [54]. As follows from Fig. 5(c), an increase in temperature up to 30 K leads to zeroing H_c. The presence of a triangular network of Fe atoms $\sqrt{3} \times \sqrt{3}$ intercalated between S-Ti-S trilayers at $x = 0.33$ as derived from the x-ray diffraction data (see above) apparently leads to the formation of a magnetic state different from that realized in $Fe_{0.25}TiS_2$ with monoclinic struture and $2\sqrt{3} \times 2 \times 2$ ordering.

As it turned out, further intercalation of Fe atoms results in the re-emergence of a jump-like magnetization change at low temperatures and a broad hysteresis loop. This can be seen in Fig. 6 which displays the temperature dependencies of the susceptibility and field dependencies of the magnetization for $Fe_{0.45}TiS_2$. In contrast to $Fe_{0.33}TiS_2$ with a trigonal structure, the $Fe_{0.45}TiS_2$ compound exhibits a monoclinic structure analogous to that observed in $Fe_{0.5}TiS_2$ (see Fig. 2) showing an AFM ground state [13–15]. Despite the presence of an AFM state, the $Fe_{0.5}TiS_2$ compound cooled at zero field below $T_N \sim 140$ K after application of a magnetic field was found to undergo to a metastable high-coercive FM state, which was confirmed by neutron diffraction and magnetoresistance measurements [13,14]. As follows from Fig. 6(a), the magnetic susceptibility of $Fe_{0.45}TiS_2$ exhibits a pronounced peak in the $\chi(T)$ dependence at $T_N \approx 135$ K, then the bifurcation of the ZFC and FC susceptibility curves upon further cooling below 100 K, and an additional hump on the ZFC susceptibility curve about 60 K. As in other Fe_xTiS_2 compounds (see above), in $Fe_{0.45}TiS_2$, the deviation of the inverse susceptibility from the expected CW behavior is detected below ~200 K [see inset in Fig. 6(a))] analogous to that observed in Fe_xTiS_2 with lower Fe concentrations. In the temperature interval 100 K $\leqslant T \leqslant$ 135 K, the $Fe_{0.45}TiS_2$ compound exhibits a metamagnetic behavior [see Fig. 6(c)], which implies

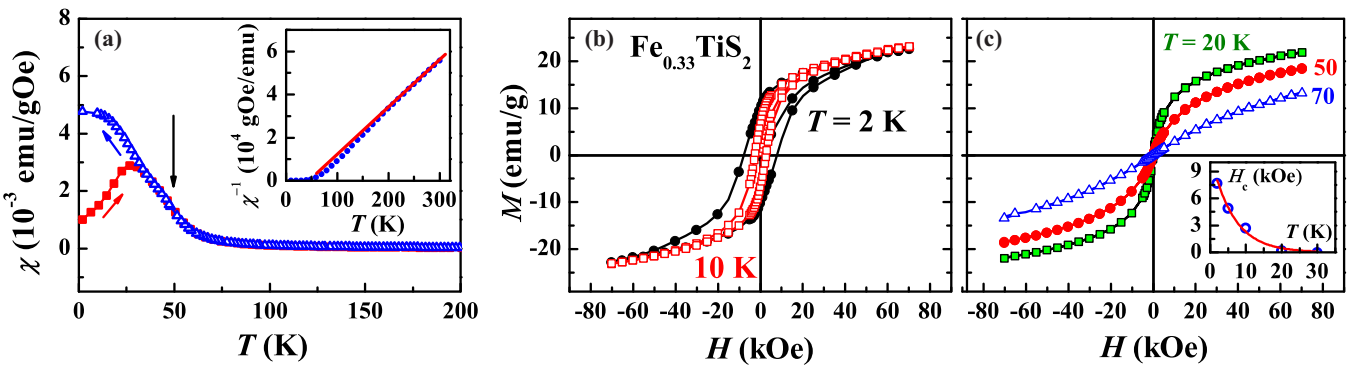

FIG. 5. Temperature dependencies of ZFC and FC magnetic susceptibilities (a) and M vs H isotherms [(b) and (c)] for $Fe_{0.33}TiS_2$. Inset shows the $\chi^{-1}(T)$ dependence.

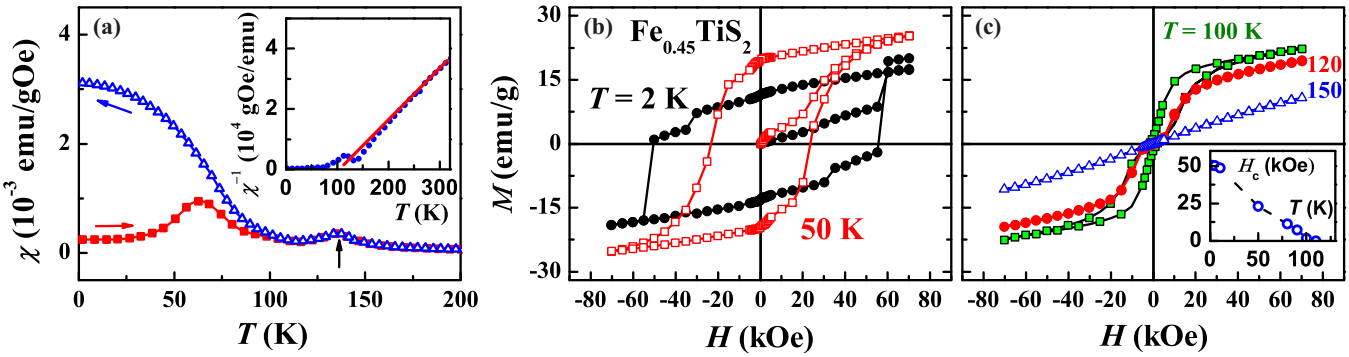

FIG. 6. ZFC and FC magnetic susceptibility at the 1 kOe field vs temperature (a) and field dependencies of the magnetization measured at various temperatures [(b) and (c)] for $Fe_{0.45}TiS_2$. Insets show the χ^{-1} and H_c vs T dependencies.

an antiferromagnetic ordering of Fe magnetic moments. A decrease in temperature below 100 K is accompanied by a significant increase in hysteresis and leads to the appearance of ferromagnetic-like hysteresis loops with a coercive force up to 50 kOe [Fig. 6(b)]. It is worth to mention that analogous temperature and field dependencies of the magnetization were observed on the $Fe_{0.5}TiS_2$ sample exhibiting the deviation from the stoichiometry after low-temperature heat treatment [13]. According to Ref. [13], the peculiar magnetic behavior of nonstoichiometric $Fe_{0.5}TiS_2$ may be associated with the presence of small regions (clusters) with the short-range FM correlations in the AFM matrix. Such an inhomogeneous magnetic state apparently exists in the $Fe_{0.45}TiS_2$ sample studied in the present work.

The $Fe_{0.75}TiS_2$ compound shows the magnetic properties (Fig. 7) that at first glance are similar to those of compounds with an iron content of about $x = 0.25$ and 0.5: (i) substantial difference in ZFC and FC susceptibility curves [see Fig. 7(a), (ii) magnetization steps on the $M(H)$ dependence at $T = 2$ K in the vicinity of H_c [Fig. 7(b)], and (iii) a fast decrease in H_c with increasing temperature [Fig. 7(c)]. However, the deviation of the inverse magnetic susceptibility behavior from the CW law is less pronounced in $Fe_{0.75}TiS_2$ in comparison with compounds with a lower Fe content; moreover, in the case of $Fe_{0.75}TiS_2$ as well as in $Fe_{0.66}TiS_2$ (see Ref. [38]), no signs of AFM ordering were found. As can be seen from Fig. 7(c), the field dependence of the magnetization at 100 K. i.e. below magnetic ordering temperature ~145 K, seems to be quite typical for a low-coercive ferromagnet or ferrimagnet. However, this behavior of the magnetization differs from that observed in the Fe_xTiS_2 compounds with $x = 0.45$ [Fig. 6(c)] and $x = 0.5$ [13] revealing metamagnetic phase transitions typical for antiferromagnets.

C. Electrical resistivity and magnetoresistance

As follows from previously reported results on the electrical properties of some Fe_xTiS_2 compounds all the samples in polycrystalline and single crystalline forms obtained by different methods with Fe concentrations $x \leqslant 0.5$ were observed to exhibit a metallic-type resistivity behavior at temperatures above 150 K [13,16,55–59]. The temperature dependencies of the relative electrical resistivity $\rho(T)/\rho_{300}$ measured at $H = 0$ and at $H = 100$ kOe on the polycrystalline samples synthesized in the present work are displayed in Fig. 8. The absolute values of ρ for our samples are in the range $(0.3–3) \times 10^{-5}$ Ohm m, which, as expected, is higher than that reported for the single crystalline samples: $(0.3–0.9) \times 10^{-5}$ Ohm m [57,60,61]. When considering the behavior of the electrical resistivity in our Fe_xTiS_2 samples, several features should be noted. There are no peculiarities on the $\rho(T)$ curves which could be associated with the formation of spin-glass or cluster glass magnetic states in compounds with low Fe concentrations ($x \leqslant 0.25$). However, for the samples with $x \geqslant 0.25$, the $\rho(T)$ dependencies demonstrate obvious anomalies in the vicinity of magnetic critical temperatures (shown by arrows

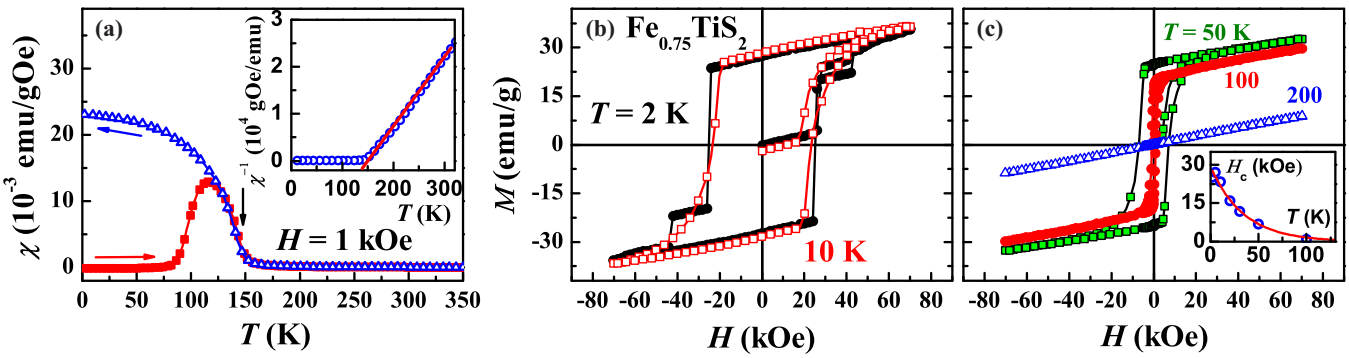

FIG. 7. Temperature dependencies of the magnetic susceptibility measured in ZFC and FC regimes (a) and $M(H)$ isotherms [(b) and (c)] measured on a $Fe_{0.75}TiS_2$ sample. Insets show the χ^{-1} and H_c vs T dependencies.

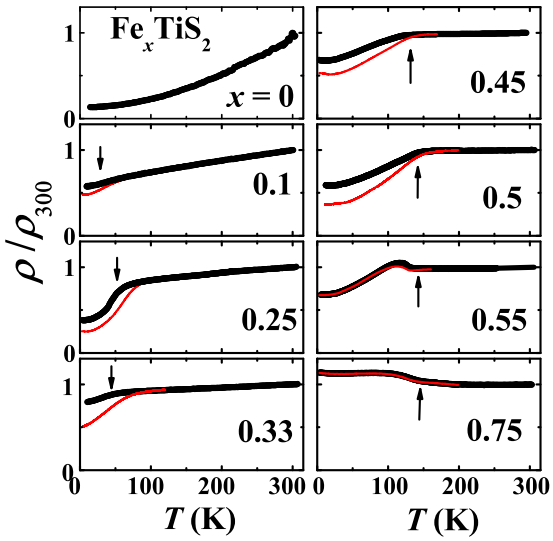

FIG. 8. Temperature dependencies of the relative electrical resistivity of the Fe_xTiS_2 polycrystalline samples measured at $H = 0$ (symbols) and at $H = 100$ kOe (line). Arrows indicate the magnetic critical temperatures.

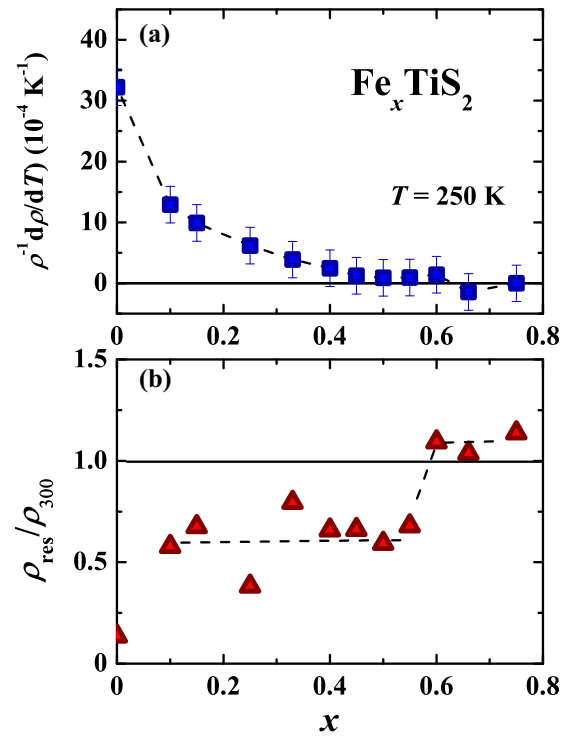

FIG. 9. Changes in the temperature coefficient of the electrical resistivity $\alpha = \rho^{-1}(d\rho/dT)$ obtained at $T = 250$ K (a) and relative residual resistivity ρ_{res}/ρ_{300} (b) with the Fe concentration in Fe_xTiS_2.

in Fig. 8). The kinks on the $\rho(T)$ curves for compounds with $0.25 \leqslant x \leqslant 0.5$ indicate that the substantial spin-dependent scattering develops in Fe_xTiS_2 with increasing temperature up to T_{crit}. Analogous changes in slope of the $\rho(T)$ dependencies around magnetic critical temperatures were observed for some single crystals of Fe_xTiS_2 [16,61]. The obtained results indicate that grain-boundary scattering does not dominate in the total resistivity of the Fe_xTiS_2 polycrystalline samples. Another feature is a change in the temperature coefficient of the electrical resistivity in the paramagnetic region with increasing Fe content. As is seen from Fig. 9(a), an increase in the Fe content results in zeroing the coefficient $\alpha = \rho^{-1}(d\rho/dT)$ obtained at $T = 250$ K, i.e., far above T_{crit}. Low α values in these compounds at $T > T_{crit}$ can be ascribed to the presence of an additional contribution to scattering of conduction electrons in the paramagnetic region. This contribution is presumably of a magnetic nature and is due to the existence of Griffith-like phase (clusters with short-range magnetic correlations) in nominally a paramagnetic state (see above). Weakening the short-range magnetic correlations and a decrease in the volume and number of such clusters with increasing temperature should decrease this contribution to the total resistivity and compensate for the increase in the phonon contribution. Moreover, as follows from Fig. 8, the behavior of the electrical resistivity below T_{crit} in compounds with the Fe contents $0.25 \leqslant x \leqslant 0.5$ differs from that observed in the samples with $x > 0.5$: the resistivity decreases with cooling below T_{crit} in the former case, while in the Fe-rich compounds ($x > 0.5$) the resistivity values in the magnetically ordered state are higher than in the paramagnetic region (at $T > T_{crit}$). To demonstrate such a discrepancy we plotted in Fig. 9 b the change in the value of the relative residual resistivity ρ_{res}/ρ_{300} as a function of the Fe content. Our value $\rho_{res}/\rho_{300} \approx 0.135$ for TiS_2 is of the same order of magnitude as that observed for single crystalline samples (see Ref. [58]). The intercalation of even small amount Fe atoms ($x \sim 0.1$) results in a substantial growth of the ρ_{res}/ρ_{300} ratio and then this ratio varies around ~0.6 with increasing Fe content up to $x = 0.55$; while further growth of Fe concentration leads to a sharp increase in the ρ_{res}/ρ_{300} ratio [see Fig. 9(b)] and substantial modifications of the $\rho(T)$ dependencies (Fig. 8). It should be emphasized that the specific shape of the $\rho(T)$ curves with an increase in $\rho(T)/\rho_{300}$ below magnetic ordering temperature and with an enhanced value of the residual resistivity is observed only in the Fe_xTiS_2 samples with the iron content above $x = 0.5$. As was mentioned above, the Fe and Ti atoms in the structure of Fe_xTiS_2 with $x \leqslant 0.5$ are well separated and located in alternating cationic layers. However, an increase in the Fe content above $x = 0.5$ is suggested to result in partial Fe-Ti mixing in the cationic layers and the appearance of magnetic inhomogeneities. The electrical resistivity of compounds with $x \geqslant 0.5$ seemingly includes an additional magnetic contribution to the resistivity from scattering of conduction electrons by such magnetic inhomogeneities in a magnetically ordered matrix below the critical temperature.

As can be seen from Fig. 8, an applied magnetic field differently affects the resistivity behavior of the Fe_xTiS_2 samples containing various amounts of Fe, which can be considered as an indication of changes in the magnetic state of compounds with increasing Fe content. Thus, the compounds with the Fe concentrations in the range $0.15 \leqslant x < 0.55$ demonstrate below critical temperature substantially reduced ρ values compared with zero field data; while for the Fe-rich samples ($x \geqslant 0.55$) the effect of an applied field of 100 kOe on the electrical resistivity is rather small.

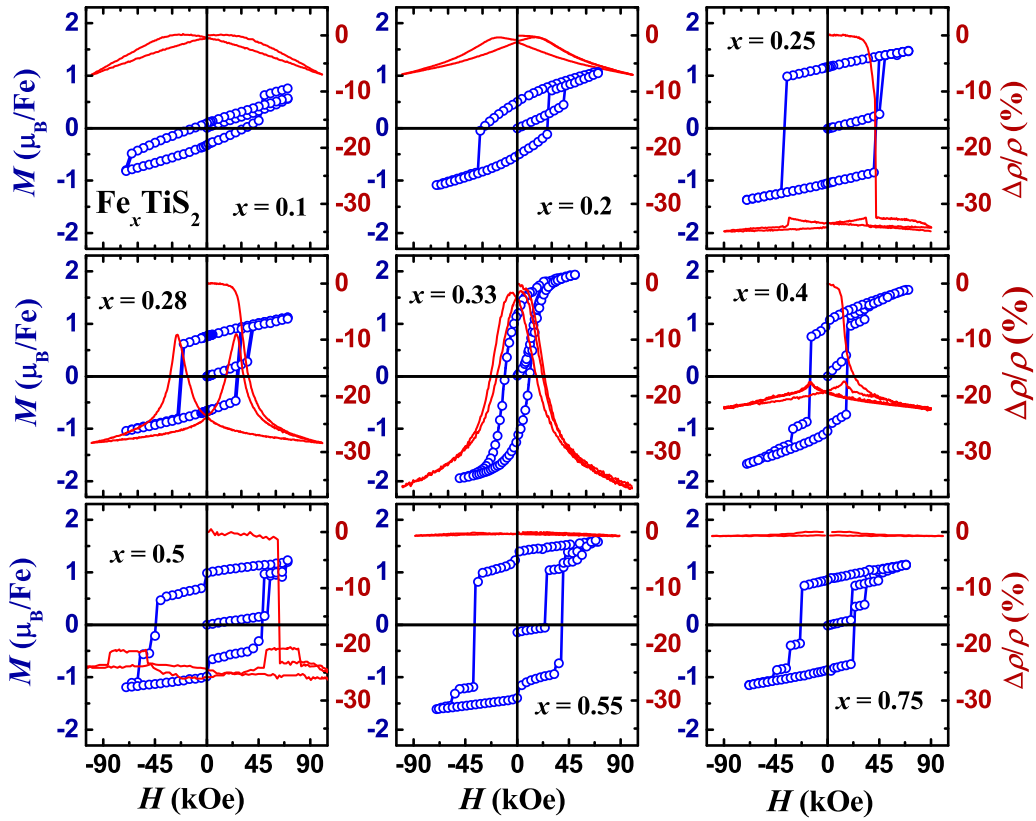

FIG. 10. Field dependencies of the magnetoresistance (lines) measured at $T = 4$ K and magnetizations (symbols) at 2 K on the Fe_xTiS_2 polycrystalline samples.

The pronounced difference in the magnetoresistance behavior observed for Fe_xTiS_2 with various Fe concentrations is clear seen in Fig. 10 which displays the field dependencies of the magnetoresistance together with magnetization isotherms. Like the $M(H)$ curves, the magnetoresistance (MR) was measured after cooling in zero field from the paramagnetic state (from 200 K) to avoid the prehistory effect on the magnetic state of the samples. For $Fe_{0.1}TiS_2$, the MR isotherm $\Delta\rho/\rho = \{[\rho(H) - \rho(0)]/\rho(0)\} \times 100$ measured at 4 K shows the hysteresis which reflects the change in the magnetization. In this sample, the applied magnetic field apparently only rotates the magnetic moments of clusters toward the field direction, which is accompanied by gradual reduction of the resistivity by about 7% in a magnetic field of ∼90kOe. After zeroing the magnetic field, the electrical resistivity of this compound is found to be only slightly lower (by ∼0.4%) than the initial (virgin) value; and the maximal $\Delta\rho/\rho$ values in $Fe_{0.1}TiS_2$ are observed at the coercive field where $M = 0$. Analogous shape of the MR curves is found for the compounds with $x = 0.15$ and $x = 0.2$, which also exhibit a cluster-glass magnetic state. This type of the magnetoresistance behavior is characteristic for magnetically inhomogeneous cluster-glass or granular systems [62].

An increase in the Fe content up to $x = 0.25$ leads to dramatic changes in the magnetoresistance behavior. While the $M(H)$ isotherms for the most Fe_xTiS_2 compounds with $x \geqslant 0.25$ look rather usual for highly anisotropic ferro- or ferrimagnets, for the samples with $0.25 \leqslant x \leqslant 0.5$, the MR behavior is clear atypical for the FM ordered materials. As follows from Fig. 10, in all these samples, the magnetic field lowers the resistivity by more than 5%; and in compounds with $x = 0.25$ and $x = 0.33$, the MR value reaches $\sim -35\%$ at $H = 100$ kOe. However, the MR isotherm for $Fe_{0.33}TiS_2$ differs substantially from that observed for the compounds with lower and higher Fe contents within range $0.25 \leqslant x \leqslant 0.5$. The compounds with $x = 0.25$, 0.28, 0.4, and 0.5 demonstrate a sharp fall in the resistivity at critical fields close to that observed on $M(H)$ isotherms (Fig. 10), nearly constant values with a further increase in the field, and large values of the remnant magnetoresistance:

$$\Delta\rho_{rem}/\rho = \{[\rho_{fin}(0) - \rho_{vgn}(0)]/\rho_{vgn}\} \times 100,$$

where ρ_{vgn} is the initial value of the electrical resistivity at $H = 0$ in the virgin magnetic state obtained after cooling the sample in zero field to a given temperature; $\rho_{fin}(0)$ is the final value of the electrical resistivity after preliminary magnetization and switching off the magnetic field.

As is seen from Fig. 10, the $\Delta\rho_{rem}/\rho$ value is close that observed in high fields. In contrary, for $Fe_{0.33}TiS_2$, the smooth $\Delta\rho/\rho$ versus field dependence without saturation is observed; and after switching off the field, the absolute remnant MR at $x = 0.33$ is found to be substantially lower ($|\Delta\rho_{rem}/\rho| \sim$ 2.5%) than the $|\Delta\rho/\rho|$ value in the 100 kOe field (∼36%).

Obviously, the difference in the magnetoresistance behavior in Fe_xTiS_2 at various Fe concentrations reflects the diversity in the magnetic state of these compounds. As was recently shown, the irreversibility of changes in $\Delta\rho/\rho$ with the magnetic field and the presence of a large remnant MR

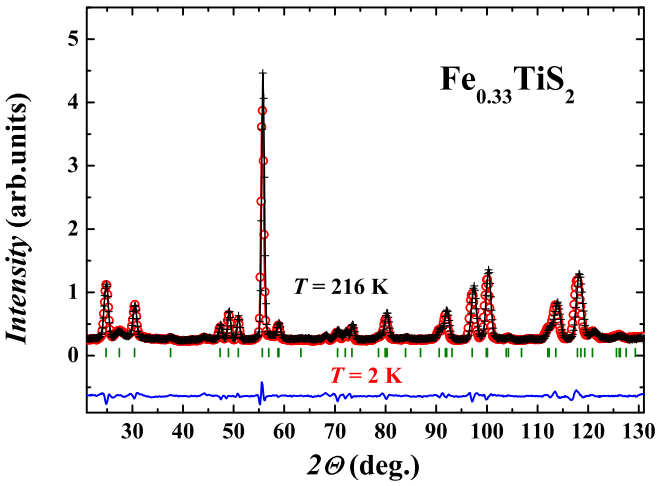

FIG. 11. Neutron diffraction patterns for $Fe_{0.33}TiS_2$ measured at $T = 216$ (crosses) and 2 K (circles). Line represents the results of the fit of the diffraction pattern at 2 K. The bottom curve shows the difference between calculated and observed 2 K intensities. The row of vertical marks below the patterns refers to the nuclear Bragg peaks corresponding to space group $P\bar{3}1c$).

in $Fe_{0.5}TiS_2$ [13,15] and $Fe_{0.25}TiS_2$ [18] is associated with the field-induced transition from the virgin AFM to the metastable FM state. In the case of $Fe_{0.5}TiS_2$, irreversibility of the AFM-FM transition at low temperatures was also confirmed by neutron diffraction measurements in magnetic fields [13,14]. As follows from Fig. 10, an increase in the Fe concentration above $x = 0.5$ leads to cardinal changes in the MR behavior; starting from $x = 0.55$ the Fe_xTiS_2 compounds with a higher iron content show very small changes in $|\Delta\rho/\rho|$ with the field that do not exceed 1%, although the field dependencies of the magnetization do not show noticeable changes.

D. Neutron diffraction for $Fe_{0.33}TiS_2$

In order to answer the question why the behavior of the magnetization and magnetoresistance in in $Fe_{0.33}TiS_2$ differs substantially from that observed in Fe_xTiS_2 compounds with lower ($x = 0.25$) and higher ($x = 0.4$–0.5) concentrations we have performed neutron diffraction measurements on a powder sample with $x = 0.33$ at 2 K, as well as at 216 K, i.e., below and above $T = 44$ K where the bifurcation of the ZFC and FC susceptibility curves was observed (see Fig. 11). As it turned out, unlike the antiferromagnetic $Fe_{0.5}TiS_2$ compound [13], the neutron powder diffraction pattern $Fe_{0.33}TiS_2$ taken at 2 K (Fig. 8) does not show additional contributions of a magnetic nature to the neutron scattering in comparison with the pattern measured at 216 K; only a small shift of the nuclear Bragg reflections is observed due changes in the lattice parameters with temperature. This observation unambiguously shows that the $Fe_{0.33}TiS_2$ compound does not exhibit a long-range magnetic order at temperatures above 2 K, and, therefore, it can be concluded that the observed changes in the susceptibility and magnetization with temperature and magnetic field (Fig. 5), and magnetoresistance (Fig. 10) are associated with the existence of a spin cluster glass state below the freezing temperature $T_f = 44$ K, as was suggested earlier from magnetic measurements (see Refs. [54,63]. It is worth to mention that previous neutron diffraction measurements performed on $Fe_{0.33}TiS_2$ [42] have revealed the appearance below 50 K of the broad diffuse maximum at low values of the scattering vector Q, which was attributed to the long-periodic short-range magnetic correlations. Apparently, the discrepancy between our neutron data and the results obtained by Y. Kuroiwa *et al.* [42] is due to the difference in sample preparation. Note that in order to achieve better sample homogeneity, long-term heat treatments were used in this work (see above). Analysis of our neutron diffraction data displayed in Fig. 8 using Le Bail fitting procedure confirmed our x-ray data (Figs. 1 and 2) that the crystal structure of $Fe_{0.33}TiS_2$ belongs to the trigonal crystal system (space group $P\bar{3}1c$), which reflects the formation of the $\sqrt{3}a_0 \times \sqrt{3}a_0$ triangular network of Fe ions in a cationic layer located between the S-Ti-S sandwiches. The presence of a such network hinders the formation of a long-range magnetic order within subsystem of the Fe magnetic moments due to frustrations of the AFM and FM exchange interactions. The existence of both FM and AFM arrangements of the Fe moments within ab plane was revealed by neutron diffraction in $Fe_{0.5}TiS_2$ [13]. Note that absence of long-range magnetic order was confirmed by neutron diffraction measurements for some other cluster-glass magnetic system with frustrated AFM and FM interactions (see Refs. [64,65], for instance).

IV. DISCUSSION AND CONCLUSION

The main magnetic and magnetoresistance data obtained in the present work are collected in Fig. 12 together with data reported in literature. As can be seen, our values of magnetic critical temperatures [Fig. 12(a)] are in good agreement with that obtained by other authors, including those for single-crystalline samples. Considering the changes in the behavior of magnetization with temperature and magnetic field, the results of the magnetoresistance studies and neutron diffraction data, several concentration ranges should be distinguished in which the magnetic state of Fe_xTiS_2 compounds differs significantly. At low Fe concentrations ($x < 0.2$), where Fe atoms are not ordered and randomly occupy octahedral positions located between the triple S-Ti-S layers, the magnetic behavior of Fe_xTiS_2 can be classified as of spin-glass and cluster-spin glass type, which is consistent with the opinion of different authors (see Refs. [9,45,46], for instance). An increase in the Fe concentration up to $x \approx 0.2$ is accompanied by a monotonous grows of the freezing temperature T_f [Fig. 12(a)]; and the magnetization and magnetoresistance behaviors with magnetic field and temperature (Figs. 3 and 10) are quite typical for materials exhibiting magnetic glassiness. As follows from the T-x diagram, further intercalation of Fe from $x = 0.25$ up to $x \sim 0.38$ is not accompanied by a remarkable increase in the magnetic critical temperature despite a reduction of the average distances between Fe atoms; moreover, at $x = 0.33$, a reduced critical temperature is determined (~44 K) than that observed in compounds with a lower Fe content (52 K and 59 K at $x = 0.25$ and $x = 0.28$, respectively). The ordering of Fe atoms and formation of the superstructure $2\sqrt{3}a_0 \times a_0 \times 2c_0$ at $x = 0.25$ results in the appearance of an AFM order below 52 K. The presence of

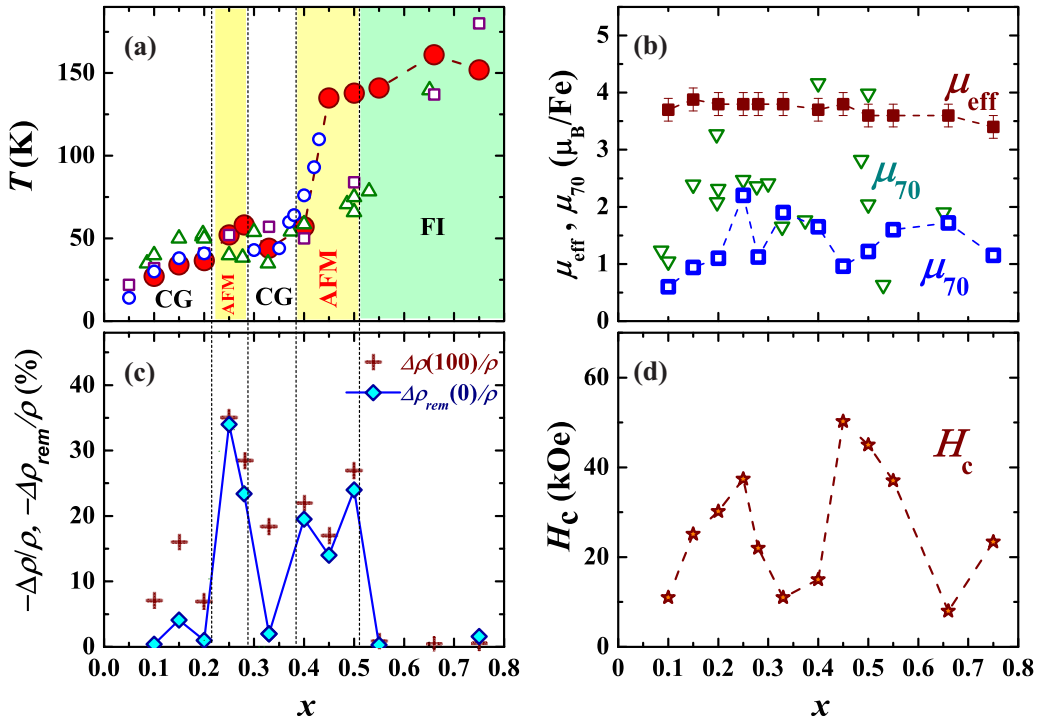

FIG. 12. (a) T-x phase diagram for the Fe_xTiS_2 (full circles: present work, up triangles: Ref. [16], open squares: Ref. [54], and open circles: Ref. [66]), (b) concentration dependencies of the magnetoresistance measured at $T = 4$ K in the 100 kOe field $\Delta\rho_{100}/\rho$ (crosses) and remnant magnetoresistance $\Delta\rho_{\rm rem}/\rho$ (diamonds); (c) variations of the effective magnetic moment $\mu_{\rm eff}$ and the magnetic moment μ_{70} in the 70 kOe field (squares: present work and down triangles: Ref. [16]) and (d) the coercive field at $T = 2$ K with the Fe content.

the AFM virgin state and irreversible field-induced AFM-FM transition in $Fe_{0.25}TiS_2$ is supported by the observation a large remnant magnetoresistance in this compound (Figs. 10 and 12). An increase in the Fe content up to $x = 0.33$ leads to the formation of the triangular network of Fe atoms, which prevents a regular arrangement of Fe magnetic moments due to frustrations of exchange interactions and results in the formation of a cluster-glass-like magnetic state. The absence of a long-range magnetic order in $Fe_{0.33}TiS_2$ is confirmed by neutron diffraction data (Fig. 11). Moreover, the field dependence of the magnetoresistance in $Fe_{0.33}TiS_2$ is found to be analogous to that observed in cluster-glass systems with low Fe concentrations ($0.1 \leqslant x \leqslant 0.2$) and is characterized by a low value of the remnant MR. A growth of the Fe content above $x = 0.4$ substantially increases the magnetic critical temperature [Fig. 12(a)]. The magnetic state of $Fe_{0.45}TiS_2$ is suggested to be inhomogeneous and consists of a matrix with a long-range AFM order with a Néel temperature of about 135 K, in which magnetic clusters with short-range magnetic correlations begin to freeze upon cooling below ~100 K; and the $Fe_{0.5}TiS_2$ compound exhibits AFM ordering in the whole temperature range below 140 K.

The large magnetoresistance ($|\Delta\rho/\rho|$ up to 35%) observed in the AFM ordered Fe_xTiS_2 compounds is attributed to the disappearance of energy gaps in the electron spectrum on the superzone boundaries under applying a magnetic field [13,15,37]. The field-induced AFM-FM transitions at low temperatures in Fe_xTiS_2 are accompanied by a large remnant MR, which indicates their irreversibility [Figs. 10 and 12(b)]. It should be noted that the irreversibility of metamagnetic transitions accompanied by remnant MR was also found in some other antiferromagnets with metallic conductivity (see Refs. [67–69]). The large value of the remnant MR observed in our Fe_xTiS_2 compounds cannot be explained by the field-induced rearrangement of the FM domains. Assuming that the realignment of the FM domains is the cause of the unusual magnetoresistance behavior in Fe_xTiS_2, a large value of the remnant MR should also be observed in compounds with $x > 0.5$, but this is not the case. It is also important to note, that in the FM and AFM ordered magnetics with very high magnetocrystalline anisotropy energy, the domain walls are narrow and do not substantially contribute to the conduction electron scattering. This follows, for example, from the MR data presented for the FM ordered Fe_xTaS_2 compounds [12,26], in which the absolute value of remnant MR does not exceed 1%. As was recently shown for $Fe_{0.5}TiS_2$ [15], the magnetoelastic interactions along with Ising-type spin states of Fe and exchange interactions may lead to irreversibility of these AFM-FM transitions and formation of a high-coercive metastable FM state in these materials. Considering the remnant magnetoresistance as a sensitive tool for detecting irreversible AFM-FM transitions the presence of two maximum on the $-(\Delta\rho_{\rm rem}/\rho)$ versus x dependence [shown in Fig. 12(b)] at $x \sim 0.25$ and $x \sim 0.5$ indicates that there is a following sequence of magnetic states in the system with increasing Fe concentration: CG → AFM → CG → AFM; in the ranges of intermediate concentrations $0.25 < x < 0.33$ and $0.33 < x < 0.5$, the magnetic state is heterogeneous with coexisting AFM and CG phases. The Fe_xTiS_2 compounds with high Fe concentrations (above $x = 0.5$) are characterized by T_C values in the range ~140–160 K, by unusual temperature dependencies of the electrical resistivity

(Figs. 8 and 9) and negligible MR values (Fig. 10). Below T_C, changes in the magnetization of the compounds with $x > 0.5$ in a magnetic field are quite typical for ferro- or ferrimagnets with high magnetocrystalline anisotropy. The fact that the electrical resistivity of Fe_xTiS_2 with $x > 0.5$ in magnetically ordered state is higher than in the disordered paramagnetic state may result from the scattering of conduction electrons by magnetic inhomogeneities appearing in the Ti layers in which some Ti ions are replaced by Fe. The presence of an additional magnetic contribution to the resistivity which does not vanish at $T \to 0$ was observed in some other metallic magnetics with substitutions (see Ref. [70], for instance). Bearing in mind the possible Fe-Ti mixing in cationic layers which can remove the compensation of Fe magnetic moments in the sublattices, the magnetic state of the compounds with $x > 0.5$ can most likely be characterized as having a ferrimagnetic (FI) order. It is worth to mention that partial mixing of Ti and Fe atoms was detected by neutron diffraction in the $Fe_4Ti_3S_8$ ($FeTi_{0.75}S_2$) compound with close metal/sulfur ratio [71]. Further neutron diffraction studies can be useful for clarifying the sequence of magnetic states in the Fe_xTiS_2 system with increasing Fe concentration, as well as for elucidating the role of Fe-Ti mixing on the behavior of magnetic and transport properties of the Fe_xTiS_2 system at a high iron content.

As derived from our magnetic susceptibility data in the temperature interval from 200 K up to 350 K, the effective magnetic moment per Fe atom in Fe_xTiS_2 varies in the range $3.4\mu_B$–$3.8\mu_B$ [Fig. 12(c)], which agrees with reported μ_{eff} values [16]. The deviation of the inverse susceptibility from the CW law observed with cooling below ~200 K in Fe_xTiS_2 with $x < 0.5$ is attributed to the presence of a Griffiths-like phase in a wide temperature range above the magnetic critical temperature. Because of the Ising-type spin state the subsystem of Fe atoms diluted with vacancies in these compounds seem to be quite compatible with the Griffiths model for random magnetic systems [51].

The values of the average magnetic moment per Fe atom in a field of 70 kOe (μ_{70}) in our polycrystalline Fe_xTiS_2 samples are determined from ~$1\mu_B$ to 2.2 μ_B; while, as shown by J. Choe *et al.* [16], for single crystalline samples, there is a significantly larger scatter of μ_{70} values determined along the easy *c* axis (from 0.63 μ_B to 4.16 μ_B). The latter may indicate the uniqueness of each Fe_xTiS_2 single crystal in terms of the distribution of iron atoms.

All the polycrystalline Fe_xTiS_2 samples studied in the present work ($0.1 \leqslant x \leqslant 0.75$) are observed to show broad hysteresis loops at low temperatures. For the compounds with ordered Fe atoms ($x \geqslant 0.25$), the values of remnant magnetization M_r are estimated to be from 0.6 μ_B to 1.4 μ_B, which is lower than ~1.45 μ_B expected for an array of single-domain ferromagnetic particles with uniaxial anisotropy [72] bearing in mind that according to the neutron diffraction data for $Fe_{0.5}TiS_2$ [13] the Fe atom possesses a magnetic moment of about 2.9 μ_B. The low-temperature coercive field of Fe_xTiS_2 is observed to vary with Fe concentration non monotonously within the range ~(10–50) kOe (Fig. 12(d)) and shows two pronounced maximums: at $x \sim 0.2$–0.25 and ~0.45–0.5. The nonmonotonic H_c versus x dependence in the Fe_xTiS_2 system was also reported earlier (see Ref. [54]). The enhanced magnetic hardness of Fe_xTiS_2 can be attributed to the presence of large unquenched orbital angular momentum on Fe atoms since according to the x-ray magnetic circular dichroism measurements Fe atoms in Fe_xTiS_2 ($0.1 \geqslant x \geqslant 0.5$) exhibit an orbital moment which varies in the range 0.25 μ_B/Fe - 0.49 μ_B/Fe [47,48]. However, we should to emphasize here that according to results of the present work and our previous studies [13–15,18] the Fe_xTiS_2 compounds with maximal H_c values are characterized as having the AFM virgin magnetic state. Therefore, along with the unquenched orbital moment of Fe, the magnetic hardness of these samples can be significantly influenced by the intrinsic exchange bias [50] since both AFM and FM interactions and their frustrations are involved in the formation of the complex magnetic behavior of Fe_xTiS_2 compounds. Further studies of the intrinsic exchange bias phenomenon in these materials are necessary for a deeper understanding of the mechanisms responsible for their magnetic hardness.

The H_c versus T dependencies observed in most Fe_xTiS_2 can be well described above 5 K by the exponential law: $H_c(T) = H_c(0)\exp(-\alpha T)$. An exponential decay of the coercive field with increasing temperature was observed in many magnetic systems with a high local magnetic anisotropy, for example, in amorphous alloys and intermetallic compounds containing rare earth elements [67,73,74], as well as in $Fe_{0.25}TaS_2$ [12]. The coercivity associated with inversions of the magnetic moments in small volumes and controlled rather by exchange interactions than the magnetocrystalline anisotropy seems to be the common feature in such materials.

In conclusion, we systematically studied the changes in the crystal structure, magnetic and transport properties with increasing Fe content in the intercalation compounds Fe_xTiS_2 synthesized by solid state reactions with prolonged homogenization heat treatments. Multiple magnetic states observed in this system are found to closely relate with the concentration of Fe atoms and their distribution over the cationic layers. This feature of the system makes each single crystal obtained with chemical vapor deposition method an almost unique object with only its inherent properties, which, we think, led to contradictions in the data on the properties of these compounds published over several decades. The results obtained in this work, such as the irreversibility of the field-induced AFM-FM transitions, the possible influence of the intrinsic exchange bias on the coercivity of Fe_xTiS_2, the presence of the Griffiths phase above the magnetic critical temperature in compounds with $x \leqslant 0.5$, as well as the unusual behavior of the electrical resistivity at $x > 0.5$, we hope, will stimulate further research in this field and in other materials.

ACKNOWLEDGMENTS

The authors are grateful to A.F. Gubkin and E.P. Proskurina for assistance in the experiments. The present work was supported by the Ministry of Education and Science The present work was supported by the Ministry of Education and Science of Russia (Project No. FEUZ-2020-0054 and theme No. AAAA-A18-118020290129-5).

[1] J. Shi, M. Hong, Z. Zhang, Q. Ji, and Y Zhang, Physical properties and potential applications of two-dimensional metallic transition metal dichalcogenides, Coord. Chem. Rev. **376**, 1 (2018).

[2] A. B. Kaul, Two-dimensional layered materials: Structure, properties, and prospects for device applications, J. Mater. Res. **29**, 348 (2014).

[3] J. Wan, S. D. Lacey, J. Dai, W. Bao, M. S. Fuhrer, and L. Hu, Tuning two-dimensional nanomaterials by intercalation: materials, properties and applications, Chem. Soc. Rev. **45**, 6742 (2016).

[4] X. Duan, C. Wang, A. Pan, R. Yu, and X. Duan, Two-dimensional transition metal dichalcogenides as atomically thin semiconductors: Opportunities and challenges, Chem. Soc. Rev. **44**, 8859 (2015)

[5] Z. Hai and S. Zhuiykov, Functionalizing New Intercalation Chemistry for Sub Nanometer Scaled Interlayer Engineering of 2D Transition Metal Oxides and Chalcogenides, Adv. Mater. Interfaces **5**, 1701385 (2018).

[6] A. D. Yoffe, Physical properties of intercalated solids, Solid State Ion. **9-10**, 59 (1983).

[7] J. A. Wilson and A. D. Yoffe, The transition metal dichalcogenides discussion and interpretation of the observed optical, electrical and structural properties, Adv. Phys. **18**, 193 (1969).

[8] S. S. P. Parkin and R. H. Friend, 3d transition-metal intercalates of the niobium and tantalum dichalcogenides. I. Magnetic properties, Philos. Mag. B **41**, 65 (1980).

[9] M. Inoue, H. P. Hughes, and A. D. Yoffe, The electronic and magnetic properties of the 3d transition metal intercalates of TiS_2, Adv. Phys. **38**, 565 (1989).

[10] N. V. Baranov, E. G. Gerasimov, and N. V. Mushnikov, Magnetism of compounds with a layered crystal structure, Phys. Metals. Metallogr. **112**, 711 (2011).

[11] N. V. Selezneva, N. V. Baranov, V. G. Pleshchev, N. V. Mushnikov, and V. I. Maksimov, Magnetic state and properties of the $Fe_{0.5}TiSe_2$ intercalation compound, Phys. Solid State **53**, 329 (2011).

[12] E. Morosan, H. W. Zandbergen, L. Li, M. Lee, J. G. Checkelsky, M. Heinrich, T. Siegrist, N. P. Ong, and R. J. Cava, Sharp switching of the magnetization in $Fe_{1/4}TaS_2$, Phys. Rev. B **75**, 104401 (2007).

[13] N. V. Baranov, E. M. Sherokalova, N. V. Selezneva, A. V. Proshkin, L. Keller, A. S. Volegov, and E. P Proskurina, Magnetic order, field induced phase transition and magnetoresistance in the intercalated compound $Fe_{0.5}TiS_2$, J. Phys.: Condens. Matter **25**, 066004 (2013).

[14] A. F. Gubkin, E. M. Sherokalova, L. Keller, N. V. Selezneva, A. V. Proshkin, E. P. Proskurina, and N. V. Baranov, Effects of S-Se substitution and magnetic field on magnetic order in $Fe_{0.5}Ti(S, Se)_2$ layered compounds, J. Alloys Compd. **616**, 148 (2014).

[15] N. V. Baranov, N. V. Selezneva, E. M. Sherokalova, Y. A. Baglaeva, A. S. Ovchinnikov, A. A. Tereshchenko, D. I. Gorbunov, A. S. Volegov, and A. A. Sherstobitov, Magnetic phase transitions, metastable states, and magnetic hysteresis in the antiferromagnetic compounds $Fe_{0.5}TiS_{2-y}Se_y$, Phys. Rev. B **100**, 024430 (2019).

[16] J. Choe, K. Lee, C. L. Huang, N. Trivedi, and E. Morosan, Magnetotransport in Fe-intercalated TS_2: Comparison between T = Ti and Ta, Phys. Rev. B **99**, 064420 (2019).

[17] N. M. Toporova, E. M. Sherokalova, N. V. Selezneva, V. V. Ogloblichev, and N. V. Baranov, Crystal structure, properties and griffiths-like phase in niobium diselenide intercalated with chromium, J. Alloys Compd. **848**, 156534 (2020).

[18] N. V. Selezneva, N. V. Baranov, E. M. Sherokalova, A. S. Volegov, and A. A. Sherstobitov, Remnant magnetoresistance and virgin magnetic state in $Fe_{0.25}TiS_2$, J. Magn. Magn. Mater. **519**, 167480 (2021).

[19] S. S. P. Parkin and R. H. Friend, 3 d transition-metal intercalates of the niobium and tantalum dichalcogenides. II. Transport properties, Philos. Mag. B **41**, 95 (1980).

[20] M. Koyano, H. Negishi, Y. Ueda, M. Sasaki, and M. Inoue, Electrical resistivity and thermoelectric power of intercalation compounds M_xTiS_2 (M = Mn, Fe, Co, and Ni), Phys. Stat. Sol. B **138**, 357 (1986).

[21] T. Moriya, and T. Miyadai, Evidence for the helical spin structure due to antisymmetric exchange interaction in $Cr_{1/3}NbS_2$, Solid State Commun. **42**, 209 (1982).

[22] Y. Tazuke. Y. Ohta, and S. Miyamoto, Exchange Interactions in Fe_xTiS_2, J. Phys. Soc. Jpn. **74**, 2644 (2005).

[23] K-T. Ko, K. Kim, S. B. Kim, H-D. Kim, J-Y. Kim, B. I. Min, J-H. Park, F-H. Chang, H-J. Lin, A. Tanaka, and S-W. Cheong, RKKY ferromagnetism with Ising-like spin states in intercalated $Fe_{0.25}TaS_2$, Phys. Pev. Lett. **107**, 247201 (2011).

[24] B. L. Morris, V. Johnson, R. H. Plovnick, and A. Wold, Magnetic properties of $FeTi_2S_4$, J. Appl. Phys. **40**, 1299 (1969).

[25] S. Muranaka, Order-disorder transition of vacancies in $FeTi_2S_4$, Mat. Res. Bull. **8**, 679 (1973).

[26] W. J. Hardy, C-W. Chen, A. Marcinkova, H. Ji, J. Sinova, D. Natelson, and E. Morosan, Very large magnetoresistance in $Fe_{0.28}TaS_2$ single crystals, Phys. Rev. B **91**, 054426 (2015).

[27] T. Miyadai, K. Kikuchi, H. Kondo, S. Sakka, M. Arai, and Y. Ishikawa, Magnetic Properties of $Cr_{13}NbS_2$, J. Phys. Soc. Jpn. **52**, 1394 (1983).

[28] V. Dyadkin, F. Mushenok, A. Bosak, D. Menzel, S. Grigoriev, P. Pattison, and D. Chernyshov, Structural disorder versus chiral magnetism in $Cr_{1/3}NbS_2$, Phys. Rev. B **91**, 184205 (2015).

[29] Y. Oka, K. Kosuge, and S. Kachi, Magnetic properties of $(Fe_xV_{1-x})V_2S_4$ and $(Fe_xV_{1-x})V_4S_8$, Mater. Res. Bull. **12**, 1117 (1977).

[30] F. Hulliger and E. V. A. Pobitschka, On the magnetic behavior of new 2H-NbS_2-type derivatives, J. Solid State Chem. **1**, 117 (1970).

[31] B. Van Laar, H. M. Rietveld, and D. J. W Ijdo, Magnetic and crystallographic structures of Me_xNbS_2 and Me_xTaS_2, J. Solid State Chem. **3**, 154 (1971).

[32] O. Gorochov, A. L. Blanc-soreau, J. Rouxel, P. Imbert, and G Jehanno, Transport properties, magnetic susceptibility and Mössbauer spectroscopy of $Fe_{0.25}NbS_2$ and $Fe_{0.33}NbS_2$, Philos. Mag. B **43**, 621 (1981).

[33] M. Shintomi, Y. Tazuke, and H. Takahashi, Structural and magnetic properties of Fe_xTiSe_2 intercalation compounds, Mol. Cryst. Liq. Cryst. **341**, 27 (2000).

[34] M. Eibschütz, S. Mahajan, F. J. DiSalvo, G. W. Hull, and J. V. Waszczak, Ferromagnetism in metallic intercalated compounds Fe_xTaS_2 ($0.20 \leqslant x \leqslant 0.34$), J. Appl. Phys. **52**, 2098 (1981).

[35] D. R. Huntley, M. J. Sienko, and K. Hiebl, Magnetic properties of iron-intercalated titanium diselenide, J. Solid State Chem. **52**, 233 (1984).

[36] S. Muranaka, and T. Takada, Growth and electrical properties of $FeMe_2X_4$ (Me = Ti, V; X = S, Se) single crystals, Bull. Inst. Chem. Res. (Kioto Univ.) **51**, 287 (1974).

[37] R. J. Elliott, and F. A. Wedgwood, Theory of the resistance of the rare earth metals, Proc. Phys. Soc. London **81**, 846 (1963).

[38] N. V. Selezneva, E. M. Sherokalova, A. S. Volegov, D. A. Shishkin, and N. V. Baranov, Crystal structure, magnetic state and electrical resistivity of $Fe_{2/3}Ti(S, Se)_2$ as affected by anionic substitutions, Mater. Res. Express **4**, 106102 (2017).

[39] F. Pawula, R. Daou, S. Hébert, O. Lebedev, A. Maignan, A. Subedi, Y. Kakefuda, N. Kawamoto, T. Baba, and T. Mori, Anisotropic thermal transport in magnetic intercalates Fe_xTiS_2, Phys. Rev. B **99**, 085422 (2019).

[40] Y. L. Chiew, M. Miyata, M. Koyano, and Y. Oshima, Clarification of the ordering of intercalated Fe atoms in Fe_xTiS_2 and its effect on the magnetic properties, Acta Cryst. B **77**, 441 (2021).

[41] Y. Kuroiwa, M. Nishimura, R. Nakajima, H. Abe, and Y. Noda, Short-range order and long-range order of Fe atoms in a spin-glass phase and a cluster-glass phase of intercalation compounds Fe_xTiS_2, J. Phys. Soc. Jpn. **63**, 4278 (1994).

[42] Y. Kuroiwa, H. Honda, and Y. Noda, Neutron Magnetic Scattering of Intercalation Compounds Fe_xTiS_2, Mol. Cryst. Liq. Cryst. **341**, 15 (2000).

[43] Y. Kuroiwa, M. Nishimura, Y. Noda, and Y. Morii, Neutron powder diffraction study of intercalation compound Fe_xTiS_2, Physica B **213**, 396 (1995).

[44] J. M. Newsam, Y. Endoh, and I. Kawada, Measurement of the cation partitionings in $Fe_xV_{3-x}S_4$ (x = 1.0 and 2.0) by powder neutron diffraction, J. Phys. Chem. Solids **48**, 607 (1987).

[45] T. Yoshioka and Y. Tazuke, Magnetic properties of Fe_xTiS_2 system, J. Phys. Soc. Jpn. **54**, 2088 (1985).

[46] M. Inoue, M. Matsumoto, H. Negishi, and H. Sakai, Low field ac magnetic susceptibility measurements of intercalation compounds M_xTiS_2 ($M = 3d$ transition metals), J. Magn. Magn. Mater. **53**, 131 (1985).

[47] A. Yamasaki, S. Imada, A. Sekiyama, S. Suga, T. Matsushita, T. Muro, Y. Saitoh, H. Negishi, and M. Sasaki, Angle-resolved photoemission spectroscopy and magnetic circular dichroism in Fe-intercalated TiS_2, Surface Rev. Lett. **9**, 961 (2002).

[48] G. Shibata, C. Won, J. Kim, Y. Nonaka, K. Ikeda, Y. Wan, M. Suzuki, T. Koide, A. Tanaka, S.-W. Cheong, and A. Fujimori, Large Orbital Magnetic Moment and Strong Perpendicular Magnetic Anisotropy in Heavily Intercalated Fe_xTiS_2, J. Phys. Chem. C. **125**, 12929 (2021).

[49] R. L. Stamps, Mechanisms for exchange bias, J. Phys. D: Appl. Phys. **33**, R247 (2000).

[50] S. Giri, M. Patra, and S. Majumdar, Exchange bias effect in alloys and compounds, J. Phys.: Condens. Matter **23**, 073201 (2011).

[51] R. B. Griffiths, Nonanalytic Behavior Above the Critical Point in a Random Ising Ferromagnet, Phys. Rev. Lett. **23**, 17 (1969).

[52] A. J. Bray, Nature of the Griffiths Phase, Phys. Rev. Lett. **59**, 586 (1987).

[53] A. H. Castro Neto, G. Castilla, and B. A. Jones, Non-Fermi Liquid Behavior and Griffiths Phase in F-Electron Compounds, Phys. Rev. Lett. **81**, 3531 (1998).

[54] H. Negishi, A. Shoube, H. Takahashi, Y. Ueda, M. Sasaki, and M. Inoue, Magnetic properties of intercalation compounds M_xTiS_2 (M = 3d transition metal), J. Magn. Magn. Mater. **67**, 179 (1987).

[55] M. Inoue, M. Koyano, H. Negishi, and Y. Ueda, Electronic properties of intercalation compound Fe_xTiS_2, J. Phys. Soc. Jpn. **55**, 1400 (1986).

[56] M. Inoue, M. Koyano, K. Fukushima, H. Negishi, and M. Sasaki, Pressure dependence of electrical resistivity in intercalation compounds M_xTiS_2 (M = 3d transition metal), Physica Stat. Sol. B **139**, 273 (1987).

[57] M. Koyano, S. Horisaka, H. Negishi, M. Sasaki, M. Inoue, N. Suzuki, and K. Motizuki, Magnetic scattering of conduction carriers in 3d transition-metal intercalates of M_xTiS_2 (M = Mn, Fe, Co, and Ni), J. Low Temp. Phys. **78**, 141 (1990).

[58] C. A. Kukkonen, W. J. Kaiser, E. M. Logothetis, B. J. Blumenstock, P. A. Schroeder, S. P. Faile, R. Colella, and J. Gambold, Transport and optical properties of $Ti_{1+x}S_2$, Phys. Rev. B **24**, 1691 (1981).

[59] H. Negishi, K. Sadahiro, S. Åhara, M. Koyano, M. Sasaki, and M. Inoue, Spin-glass behavior in itinerant magnetic material of Fe_xTiS_2, J. Magn. Mag. Mater. **90**, 345 (1990).

[60] M. Danot, J. Rouxel, and O. Gorochov, Proprietes electriques, magnetiques et structurales des phases M_xTiS_2 (M = Fe, Co, Ni), Mat. Res. Bull. **9**, 1383 (1974).

[61] M. Inoue, M. Marushita, H. Negishi, and M. Koyano, Point-contact spectroscopy for itinerant-magnetic material of Fe_xTiS_2, J. Low Temp. Phys. **73**, 469 (1988).

[62] J. Q. Xiao, J. S. Jiang, and C. L. Chien, Giant Magnetoresistance in Nonmultilayer Magnetic Systems, Phys. Rev. Lett. **68**, 3749 (1992).

[63] M. Koyano, M. Suezawa, H. Watanabe, and M. Inoue, Low-field magnetization and ac magnetic susceptibility of spin-and cluster-glasses of itinerant magnet Fe_xTiS_2, J. Phys. Soc. Jpn. **63**, 1114 (1994).

[64] A. F. Gubkin, E. A. Sherstobitova, P. B. Terentyev, A. Hoser, and N. V. Baranov, A cluster-glass magnetic state in R_5Pd_2 (R= Ho, Tb) compounds evidenced by AC-susceptibility and neutron scattering measurements, J. Phys: Condens. Matter. **25**, 236003 (2013).

[65] I. M. Siouris, S. Katsavounis, V. Kontopou, A. Hoser, and R. K. Kremer, Cluster glass transition in the ternary Dy_2AgIn_3 system determined by neutron diffraction and Ac-Dc magnetization measurements, J. Magn. Magn. Mater. **514**, 167123 (2020).

[66] T. Satoh, Y. Tazuke, M. Tomonao, and H. Kensuke, Ferromagnetic and reentrant spin glass properties in an Ising magnet Fe_xTiS_2, J. Phys. Soc. Jpn. **57**, 1743 (1988).

[67] A. F. Gubkin, L. S. Wu, S. E. Nikitin, A. V. Suslov, A. Podlesnyak, O. Prokhnenko, K. Proke Å¡, F. Yokaichiya, L. Keller, and N. V. Baranov, Field-induced magnetic phase transitions and metastable states in Tb_3Ni, Phys. Rev. B **97**, 134425 (2018).

[68] N. V. Baranov, E. Bauer, R. Hauser, A. Galatanu, Y. Aoki, and H. Sato, Field-induced phase transitions and giant magnetoresistance in Dy_3Co single crystals, Eur. Phys. J. B **16**, 67 (2000).

[69] K. Sengupta, and E. V. Sampathkumaran, Field-induced first-order magnetic phase transition in an intermetallic compound Nd_7Rh_3: Evidence for kinetic hindrance, phase coexistence, and percolative electrical conduction, Phys. Rev. B **73**, 020406(R) (2006).

[70] J. Stankiewicz, J. Bartolomé, and D. Fruchart, Spin Disorder Scattering in Magnetic Metallic Alloys, Phys. Rev. Lett. **89**, 106602 (2002).

[71] N. V. Baranov, P. N. G. Ibrahim, N. V. Selezneva, A. F. Gubkin, A. S. Volegov, D. A. Shishkin, L. Keller, D. Sheptyakov, and E. A. Sherstobitova, Layer-preferential substitutions and magnetic properties of pyrrhotite-type $Fe_{7-y}M_yX_8$ chalcogenides (X = S, Se; M = Ti, Co), J. Phys: Condens. Matter. **27**, 286003 (2015).

[72] J. M. D. Coey, *Magnetism and Magnetic Materials* (Cambridge University Press, Cambridge, 2010).

[73] J. M. D. Coey, T. R. McGuire, and B. Tissier, Amorphous Dy-Cu: random spin freezing in the presence of strong local anisotropy, Phys. Rev. B **24**, 1261 (1981).

[74] N. V. Baranov, V. I. Pushkarski, A. E. Sviderski, and H. Sassik, Magnetic properties of liquid quenched R_3Co alloys, J. Magn. Magn. Mater. **157**, 635 (1996).